Chimeric γPNA-Invader probes: Using intercalator-functionalized oligonucleotides to enhance the DNA-targeting properties of γPNA

Raymond G. Emehiser and Patrick J. Hrdlicka.

Department of Chemistry, University of Idaho, Moscow, ID-83844, USA

E-mail: hrdlicka@uidaho.edu

ELECTRONIC SUPPLEMENTARY INFORMATION

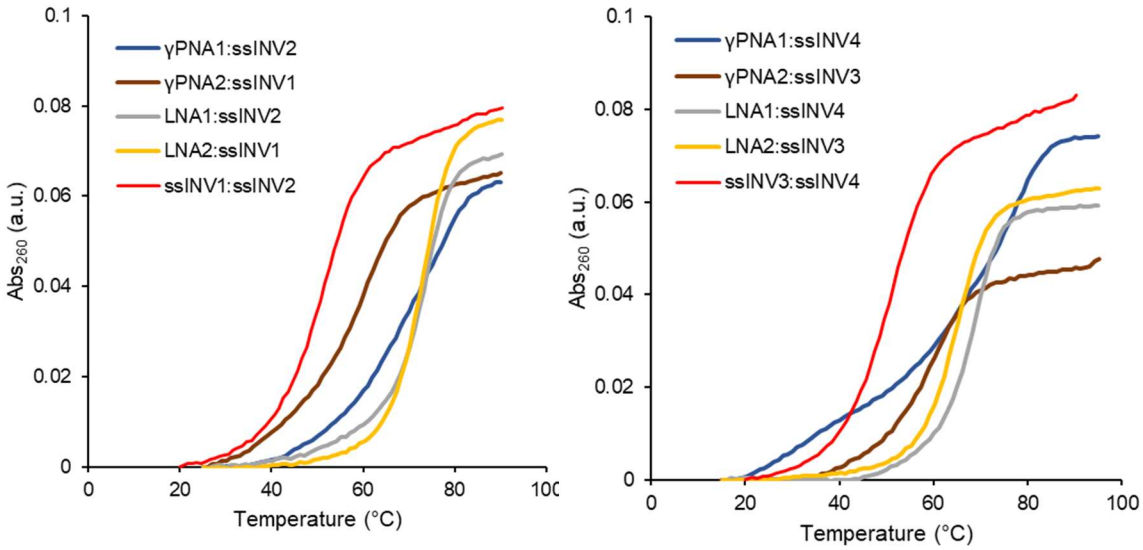

Figure S1. Representative thermal denaturation curves of chimeric γPNA-Invader and LNA-Invader duplexes. For experimental conditions, see Table 1. Thermal denaturation curves for the studied duplexes between individual Invader, γPNA or LNA strands and cDNA have been reported in reference S2.

Additional discussion regarding the dsDNA-recognition potential of probes studied herein. The *TA*-based conclusions concerning the dsDNA-recognition potential of the different probes (Table 1 and Table S1) are similar to the $\Delta G_{\mathrm{rec}}^{310}$-based conclusions (Table 2 and Table S2). Thus, chimeric γPNA-Invader probes display very prominent dsDNA-recognition potential as evidenced by *TA* values in excess of 33.5 °C (note *TA* values for entries 1-4, Table 1). This is primarily due to the very high stability of the probe:cDNA duplexes vis-à-vis the unmodified dsDNA duplexes, whereas the rather stable nature of the chimeric γPNA-Invader probes partially reduces the dsDNA-recognition potential. The chimeric LNA-Invader probes display more limited dsDNA-recognition potential as discussion evidenced by the low *TA* values (≤ 16.5 °C, entries 5-8, Table 1). This is largely due to the high stability of the LNA-Invader probe duplexes. Although the driving force likely could be increased by using more extensively modified LNA strands, which induce more prominent *A*-type preorganization and display progressively reduced affinity towards intercalator-functionalized ONs[S1] and increased affinity towards cDNA, we did not pursue this option in the present study. As previously reported,[S2] conventional Invader probes display prominent dsDNA-recognition potential (*TA* ~35 °C, entries 1 and 2, Table S1). Single-stranded γPNA probes also display high dsDNA-targeting potential (*TA* ≥ 41.5 °C, entries 3 and 4, Table S1), whereas LNA-modified ONs display moderate dsDNA-targeting potential (*TA* = 16.5-17.5 °C, entries 5 and 6, Table S1)

The favorable $\Delta G_{\mathrm{rec}}^{310}$ values calculated for dsDNA-recognition using chimeric γPNA-Invader probes (Table 2) is a consequence of exceptionally favorable changes in enthalpy (ΔH_{rec} between -429 kJ/mol and -369 kJ/mol, entries 1-4, Table S3), which are partially offset by unfavorable entropic contributions ($-T\Delta S_{rec}^{310}$ between 285 kJ/mol and 340 kJ/mol, entries 1-4, Table S4). This, in turn, is a manifestation of enthalpically destabilized probe duplexes ($\Delta\Delta H$

between +78 kJ/mol to +194 kJ/mol, entries 1-4, Table S3) and enthalpically stabilized duplexes between individual probe strands and cDNA ($\Delta\Delta H$ between -167 kJ/mol to -82 kJ/mol, entries 1-4, Table S3). The enthalpically labile nature of the chimeric γPNA-Invader probes is consistent with our expectation that γPNA probes display reduced compatibility with intercalator-modified ONs. In fact, chimeric γPNA-Invader probes are far more strongly enthalpically activated for dsDNA-recognition than single-stranded γPNA probes (ΔH_{rec} for **γPNA2** = -167 kJ/mol, entry 12, Table S3) or conventional Invader probes (ΔH_{rec} between -321 and -299 kJ/mol, entries 9-10, Table S3).

In contrast, the chimeric LNA-Invader probes are only moderately enthalpically activated for dsDNA-recognition (ΔH_{rec} between -207 to -67 kJ/mol, Table S3), mainly because the probe duplexes, with one exception, are enthalpically stabilized ($\Delta\Delta H$ between -114 to +59 kJ/mol, Table S3). As discussed above, it appears that higher LNA modification levels are necessary to sufficiently destabilize chimeric probe duplexes. Single-stranded LNAs are even more weakly enthalpically activated for dsDNA-recognition (ΔH_{rec} between -110 to -66 kJ/mol, Table S3).

Table S1. Sequences of probes studied herein, T_m*s* of probe duplexes and duplexes between individual probe strands and cDNA, and *TA* values.[a]

Entry	Probes	Sequences	T_m [ΔT_m] (°C) probe duplex	T_m [ΔT_m] (°C) upper strand vs cDNA	T_m [ΔT_m] (°C) lower strand vs cDNA	*TA* (°C)
1	**ssINV1** **ssINV2**	5'-GG**X** ATA **X**A**X** AGG C 3'-CCA **X**AT A**X**A **X**CC G	52.0 [+14.5]	61.5 [+24.0]	62.5 [+25.0]	+34.5
2	**ssINV3** **ssINV4**	5'-GG**X** A**X**A TA**X** AGG C 3'-CCA **X**A**X** ATA **X**CC G	51.0 [+13.5]	61.0 [+23.5]	63.0 [+25.5]	+35.5
3	**γPNA1**	H-Lys-GGT ATA TAT AGG C-Lys-NH_2	-	>85 [>47.5]	-	>47.5
4	**γPNA2**	NH_2-Lys-CCA TAT ATA TCC G-Lys-H	-	-	79.0 [+41.5]	+41.5
5	**LNA1**	5'-GgT AtA TaT AgG C	-	54.0 [+16.5]	-	+16.5
6	**LNA2**	3'-CCa TAt ATa TCc G	-	-	55.0 [+17.5]	+17.5

[a]LNA monomers are denoted by lower case letters ("c" = 5-methylcytosine LNA monomer). ΔT_m = change in T_m relative to the unmodified DNA duplex, T_m (5'-GGTATATATAGGC:3'-CCATATATATCCG) = 37.5 °C. For a definition of *TA*, see the main text. For experimental conditions, see Table 1. Data points have been previously reported in reference S2 and are listed here for the reader's convenience.

Table S2. Change in Gibbs free energy at 310 K (ΔG^{310}) upon formation of probe duplexes, and duplexes between individual probe strands and cDNA. Also shown is the calculated change in reaction free energy upon probe-mediated recognition of isosequential dsDNA targets ($\Delta G^{310}_{\mathrm{rec}}$).[a]

Entry	Probes	Sequences	ΔG^{310} [$\Delta\Delta G^{310}$] (kJ/mol)			ΔG^{310}_{rec} (kJ/mol)
			probe duplex	upper strand vs cDNA	lower strand vs cDNA	
1	**ssINV1** **ssINV2**	5'-GG**X** ATA **X**A**X** AGG C 3'-CCA **X**AT A**X**A **X**CC G	-53 [-12]	-80 [-38]	-76 [-34]	-60
2	**ssINV3** **ssINV4**	5'-GG**X** A**X**A TA**X** AGG C 3'-CCA **X**A**X** ATA **X**CC G	-53 [-11]	-78 [-36]	-78 [-37]	-62
3	**γPNA1**	H-Lys-GGT ATA TAT AGG C-Lys-NH_2	-	nd	-	nd
4	**γPNA2**	NH_2-Lys-CCA TAT ATA TCC G-Lys-H	-	-	-109 [-67]	-67
5	**LNA1**	5'-GgT AtA TaT AgG C	-	-63 [-21]	-	-21
6	**LNA2**	3'-CCa TAt ATa TCc G	-	-	-68 [-26]	-26

[a] $\Delta\Delta G^{310}$ is determined relative to the corresponding unmodified DNA duplex (ΔG^{310} = -42 kJ/mol). For a definition of $\Delta G^{310}_{\mathrm{rec}}$, see the main text. For enthalpic and entropic parameters, see Tables S3 and S4. nd = not determined due to unclear baseline. For experimental conditions, see Table 1. Data points have been previously reported in reference S2 and are listed here for the reader's convenience.

Table S3. Change in enthalpy (ΔH) upon formation of probe duplexes, and duplexes between individual probe strands and cDNA. Also shown is the calculated change in reaction enthalpy upon probe-mediated recognition of the isosequential dsDNA target (ΔHrec).[a]

Entry	Probes	Sequences	ΔH [$\Delta\Delta H$] (kJ/mol)			ΔH_{rec} (kJ/mol)
			probe duplex	upper strand vs cDNA	lower strand vs cDNA	
1	**γPNA1** **ssINV2**	H-Lys-GGT ATA TAT AGG C-Lys-NH_2 3'-CCA **X**AT A**X**A **X**CC G	-231 [+194]	nd	-508 [-82]	nd
2	**ssINV1** **γPNA2**	5'-GG**X** ATA **X**A**X** AGG C NH_2-Lys-CCA TAT ATA TCC G-Lys-H	-307 [+118]	-569 [-143]	-593 [-167]	-429
3	**γPNA1** **ssINV4**	H-Lys-GGT ATA TAT AGG C-Lys-NH_2 3'-CCA **X**A**X** ATA **X**CC G	-309 [+116]	nd	-541 [-115]	nd
4	**ssINV3** **γPNA2**	5'-GG**X** A**X**A TA**X** AGG C NH_2-Lys-CCA TAT ATA TCC G-Lys-H	-348 [+78]	-550 [-124]	-593 [-167]	-369
5	**LNA1** **ssINV2**	5'-GgT AtA TaT AgG C 3'-CCA **X**AT A**X**A **X**CC G	-366 [+59]	-491 [-66]	-508 [-82]	-207
6	**ssINV1** **LNA2**	5'-GG**X** ATA **X**A**X** AGG C 3'-CCa TAt ATa TCc G	-537 [-112]	-569 [-143]	-535 [-110]	-122
7	**LNA1** **ssINV4**	5'-GgT AtA TaT AgG C 3'-CCA **X**A**X** ATA **X**CC G	-539 [-114]	-491 [-66]	-541 [-115]	-67
8	**ssINV3** **LNA2**	5'-GG**X** A**X**A TA**X** AGG C 3'-CCa TAt ATa TCc G	-457 [-31]	-550 [-124]	-535 [-110]	-203
9	**ssINV1** **ssINV2**	5'-GG**X** ATA **X**A**X** AGG C 3'-CCA **X**AT A**X**A **X**CC G	- 352 [+73]	-569 [-143]	-508 [-82]	-299
10	**ssINV3** **ssINV4**	5'-GG**X** A**X**A TA**X** AGG C 3'-CCA **X**A**X** ATA **X**CC G	-344 [+81]	-550 [-124]	-541 [-115]	-321
11	**γPNA1**	H-Lys-GGT ATA TAT AGG C-Lys-NH_2	-	nd	-	nd
12	**γPNA2**	NH_2-Lys-CCA TAT ATA TCC G-Lys-H	-	-	-593 [-167]	-167
13	**LNA1**	5'-GgT AtA TaT AgG C	-	491 [-66]	-	-66
14	**LNA2**	3'-CCa TAt ATa TCc G	-	-	-535 [-110]	-110

[a] $\Delta\Delta H$ is determined relative to the corresponding unmodified DNA duplex (ΔH = -426 kJ/mol). ΔH_{rec} = ΔH (upper probe vs cDNA) + ΔH (lower probe vs cDNA) - ΔH (probe) - ΔH (dsDNA). nd = not determined due to unclear baseline. For experimental conditions, see Table 1. Data points for entries in "upper strand vs cDNA" and "lower strand vs cDNA" columns, as well as data points listed in the "probe duplex" column for entries 9 and 10, have previously been reported in reference S2, and are listed here for the reader's convenience.

Table S4. Change in entropy at 310 K ($-T\Delta S^{310}$) upon formation of probes duplexes, and duplexes between individual probe strands and cDNA. Also shown is the calculated change in reaction entropy at 310 K upon probe-mediated recognition of the isosequential dsDNA target ($-T\Delta S^{310}_{rec}$).[a]

Entry	Probes	Sequences	$-T\Delta S^{310}$ [$\Delta(T\Delta S^{310})$] (kJ/mol)			$-T\Delta S^{310}_{rec}$ (kJ/mol)
			probe duplex	upper strand vs cDNA	lower strand vs cDNA	
1	**γPNA1** **ssINV2**	H-Lys-GGT ATA TAT AGG C-Lys-NH_2 3'-CCA **X**AT A**X**A **X**CC G	172 [-211]	nd	432 [+49]	nd
2	**ssINV1** **γPNA2**	5'-GG**X** ATA **X**A**X** AGG C NH_2-Lys-CCA TAT ATA TCC G-Lys-H	249 [-134]	489 [+105]	484 [+100]	+340
3	**γPNA1** **ssINV4**	H-Lys-GGT ATA TAT AGG C-Lys-NH_2 3'-CCA **X**A**X** ATA **X**CC G	238 [-146]	nd	462 [+79]	nd
4	**ssINV3** **γPNA2**	5'-GG**X** A**X**A TA**X** AGG C NH_2-Lys-CCA TAT ATA TCC G-Lys-H	287 [-97]	472 [+88]	484 [+100]	+285
5	**LNA1** **ssINV2**	5'-GgT AtA TaT AgG C 3'-CCA **X**AT A**X**A **X**CC G	294 [-89]	428 [+44]	432 [+49]	+182
6	**ssINV1** **LNA2**	5'-GG**X** ATA **X**A**X** AGG C 3'-CCa TAt ATa TCc G	445 [+61]	489 [+105]	468 [+84]	+111
7	**LNA1** **ssINV4**	5'-GgT AtA TaT AgG C 3'-CCA **X**A**X** ATA **X**CC G	451 [+67]	428 [+44]	462 [+79]	+55
8	**ssINV3** **LNA2**	5'-GG**X** A**X**A TA**X** AGG C 3'-CCa TAt ATa TCc G	382 [-2]	472 [+88]	468 [+84]	+174
9	**ssINV1** **ssINV2**	5'-GG**X** ATA **X**A**X** AGG C 3'-CCA **X**AT A**X**A **X**CC G	299 [-85]	489 [+105]	432 [+49]	+239
10	**ssINV3** **ssINV4**	5'-GG**X** A**X**A TA**X** AGG C 3'-CCA **X**A**X** ATA **X**CC G	292 [-92]	472 [+88]	462 [+79]	+258
11	**γPNA1**	H-Lys-GGT ATA TAT AGG C-Lys-NH_2	-	nd	-	nd
12	**γPNA2**	NH_2-Lys-CCA TAT ATA TCC G-Lys-H	-	-	484 [+100]	+100
13	**LNA1**	5'-GgT AtA TaT AgG C	-	428 [+44]	-	+44
14	**LNA2**	3'-CCa TAt ATa TCc G	-	-	468 [+84]	+84

[a] $\Delta(T\Delta S^{310})$ is measured relative to the corresponding unmodified DNA duplex ($-T\Delta S^{310}$ = 384 kJ/mol). $-T\Delta S^{310}_{rec}$= $\Delta(T^{310}\Delta S)$ (upper probe vs cDNA) + $\Delta(T^{310}\Delta S)$ (lower probe vs cDNA) - $\Delta(T^{310}\Delta S)$ (probe). nd = not determined due to unclear baseline. For experimental conditions, see Table 1. Data points for entries in "upper strand vs cDNA" and "lower strand vs cDNA" columns, as well as data points listed in the "probe duplex" column for entries 9 and 10, have previously been reported in reference S2, and are listed here for the reader's convenience.

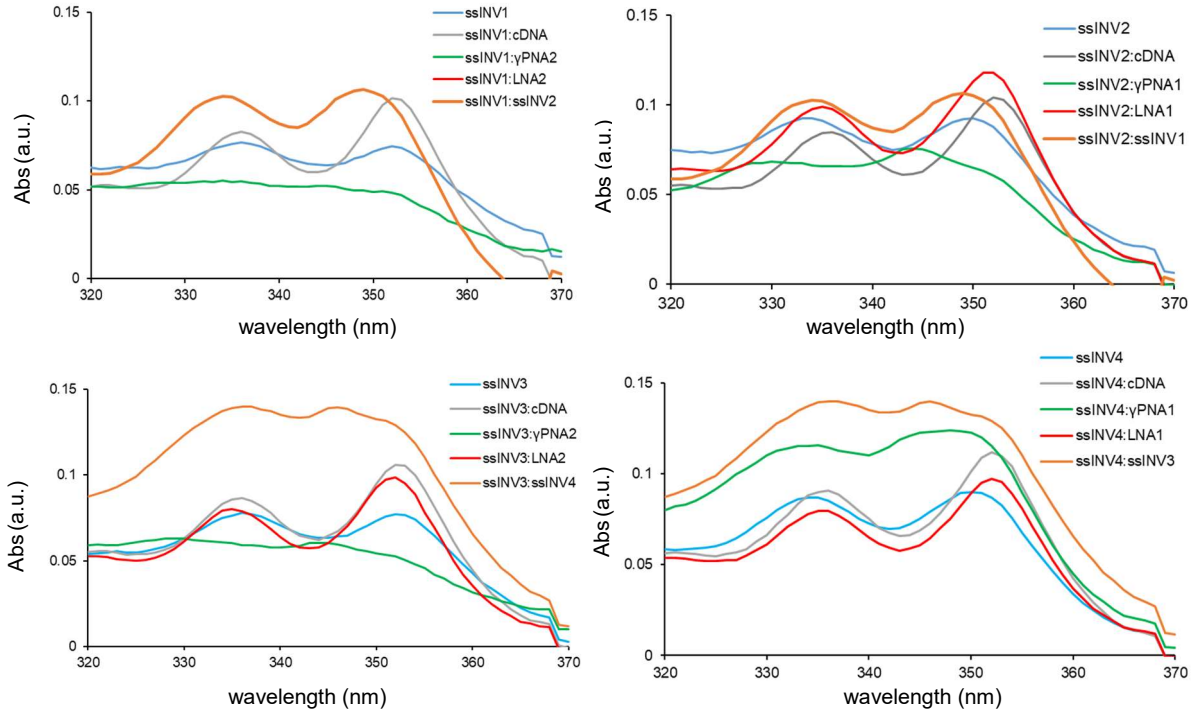

Figure S2. UV-Vis absorption spectra for single-stranded Invader probes **ssINV1-ssINV4** and the corresponding duplexes with complementary DNA, γPNA, LNA, and Invader strands. Spectra were recorded at T = 10 °C in T_m buffer using quartz optical cells with a 1.0 cm path-length.

Table S5. Absorption maxima in the 340-365 nm region for single-stranded Invader probes and the corresponding duplexes with complementary DNA, γPNA, LNA or Invader strands.[a]

	λ_{max} (nm) [$\Delta\lambda_{max}$]				
Probe	**SSP**	**+cDNA**	**+ γPNA**	**+LNA**	**+ssINV**
ssINV1	352	352 [±0]	344 [-8]	352 [±0]	349 [-3]
ssINV2	350	352 [+2]	344 [-6]	352 [+2]	349 [-1]
ssINV3	352	352 [±0]	344 [-8]	352 [±0]	346 [-6]
ssINV4	349	352 [+3]	348 [-1]	352 [+3]	346 [-3]

[a] SSP = single-stranded probe. $\Delta\lambda_{max}$ is calculated relative to the single-stranded Invader strand. Binding partners (listed in the parenthesis) are as follows **ssINV1** (**γPNA2**, **LNA2**, **ssINV2**), **ssINV2** (**γPNA1**, **LNA1**, **ssINV1**), **ssINV3** (**γPNA1**, **LNA1**, **ssINV1**), and **ssINV4** (**γPNA1**, **LNA1**, **ssINV1**). Measurements were performed at 10 °C in T_m buffer using quartz optical cells with a 1.0 cm path length.

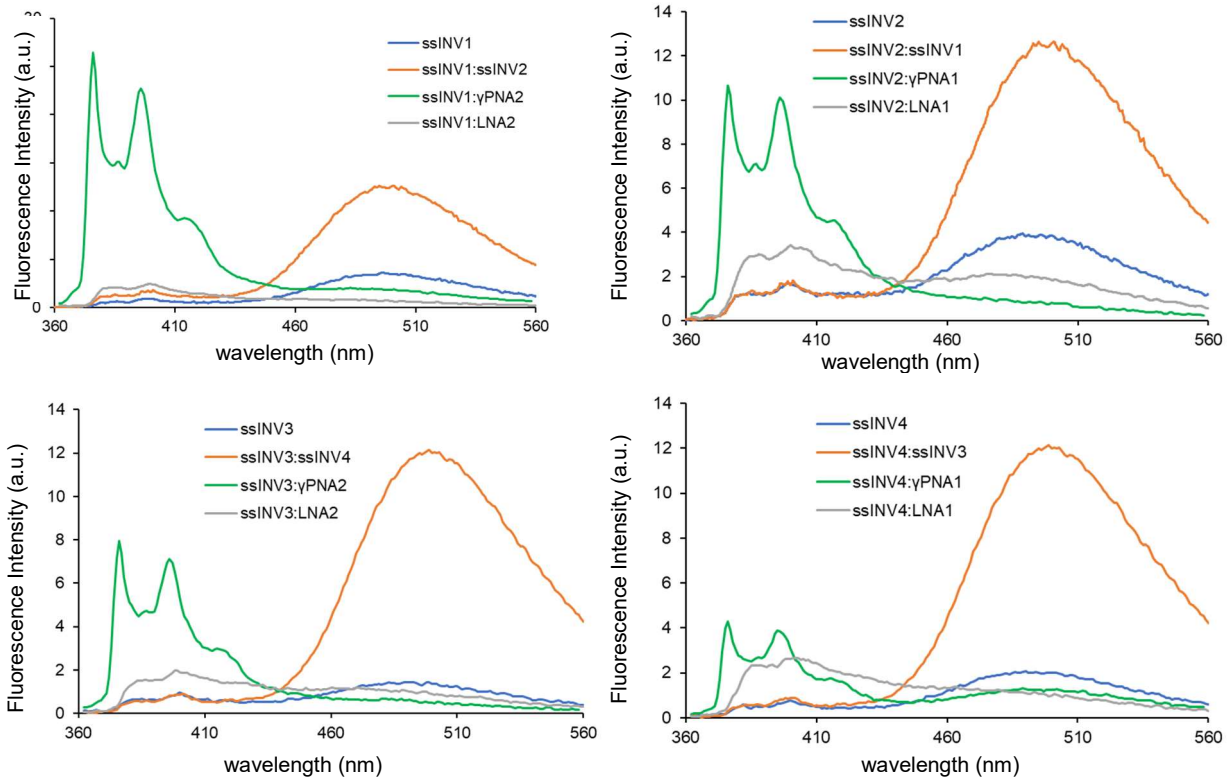

Figure S3. Steady-state fluorescence emission spectra for single-stranded Invader probes **ssINV1-ssINV4** and the corresponding duplexes with complementary γPNA, LNA, and Invader strands. Spectra were recorded at $T = 5$ °C in T_m buffer using $\lambda_{ex} = 350$ nm and quartz optical cells with a 1.0 cm path-length.

Table S6. I_5/I_1 ratios for single-stranded Invader probes and duplexes with complementary DNA, γPNA, LNA, or Invader strands.[a]

	I_5/I_1 ratios			
Probe	**SSP**	**+ γPNA**	**+LNA**	**+ssINV**
ssINV1	1.5	0.9	1.2	1.5
ssINV2	1.3	0.9	1.2	1.5
ssINV3	1.3	0.9	1.3	1.5
ssINV4	1.5	0.9	1.1	1.5

[a] SSP = single-stranded Invader probe. Binding partners (listed in the parenthesis) are as follows **ssINV1** (**γPNA2**, **LNA2**, **ssINV2**), **ssINV2** (**γPNA1**, **LNA1**, **ssINV1**), **ssINV3** (**γPNA2**, **LNA2**, **ssINV4**), and **ssINV4** (**γPNA1**, **LNA1**, **ssINV3**). I_5/I_1 ratios were calculated based on observed emission maxima in the 396-401 nm range for I_5 and 378-383 nm range for I_1. Measurements were performed at 5 °C in T_m buffer using quartz optical cells with a 1.0 cm path-length.

Additional discussion regarding the nature of the recognition complexes formed between DH1 and chimeric γPNA-Invader probes. Additional experiments were performed to verify that incubation of the chimeric **γPNA1**:**ssINV2** probe with **DH1** indeed results in the formation of a **γPNA1**:**DH1**:**ssINV2** complex and not the ternary **DH1**:(**γPNA1**)$_2$-complex seen when **γPNA1** is incubated with **DH1** (i.e., compare lanes 2 and 6 in Fig. 5 in the main manuscript). Towards this end, **γPNA1** and **γPNA2** were incubated with 36-mer DIG-labeled single-stranded DNA targets **ON1** or **ON2** as previously reported[S2] (sequences listed in Fig. S4). These targets have the same length as **DH1** and feature i) a central T_{10} region, ii) a complementary or isosequential arm relative to the γPNA strand, and iii) a scrambled arm. As expected, evidence for formation of a duplex with a long single-stranded overhang is observed when **ON1** and **γPNA2** or **ON2** and **γPNA1** are incubated (compare lanes 5 and 1, and lanes 4 and 8, Fig. S4). There are no signs of duplex formation between **ON2** and **γPNA2** (compare lanes 5 and 7), whereas **ON1** and **γPNA1**, unexpectedly, appear to form a double-stranded structure (compare lanes 4 and 2), which we have previously argued reflects formation of an anti-parallel 8-mer duplex across the AT-rich region, with 2 and 3 nt single-stranded overhangs (for illustration, see Fig. S4).[S2] This, in turn, prompted us to suggest that the slower-moving band seen when an excess of **γPNA1** is incubated with **DH1** (annealing conditions: lane 3, Fig. S4, and non-annealing conditions: lane 6, Fig. 5) represents the aforementioned ternary **DH1**:(**γPNA1**)$_2$-complex in which two **γPNA1** strands are bound to **DH1**, both binding in anti-parallel orientation, one strand binding to the fully complementary 13-mer region and the other strand binding to the complementary 8-mer region.

Importantly, the main recognition bands seen when the chimeric **γPNA1**:**ssINV2** or **γPNA2**:**ssINV1** probes are incubated with **DH1**, display i) slightly reduced mobility vis-à-vis the recognition bands from the **γPNA1**:**ON2** and **γPNA2**:**ON1** duplexes (compare lanes 6 and 1, and

lanes 10 and 8, Fig. S4), and ii) increased mobility relative to the ternary **DH1**:(**γPNA1**)$_2$-complex (compare lanes 6 and 10 with lane 3, Fig. S4). These observations are consistent with the formation of a complex entailing **DH1**, a γPNA strand, and a single-stranded Invader strand when **DH1** is incubated with chimeric γPNA-Invader probes (i.e., **γPNA1**:**DH1**:**ssINV2**, **γPNA2**:**DH1**:**ssINV1**, **γPNA1**:**DH1**:**ssINV4**, and **γPNA2**:**DH1**:**ssINV3**).

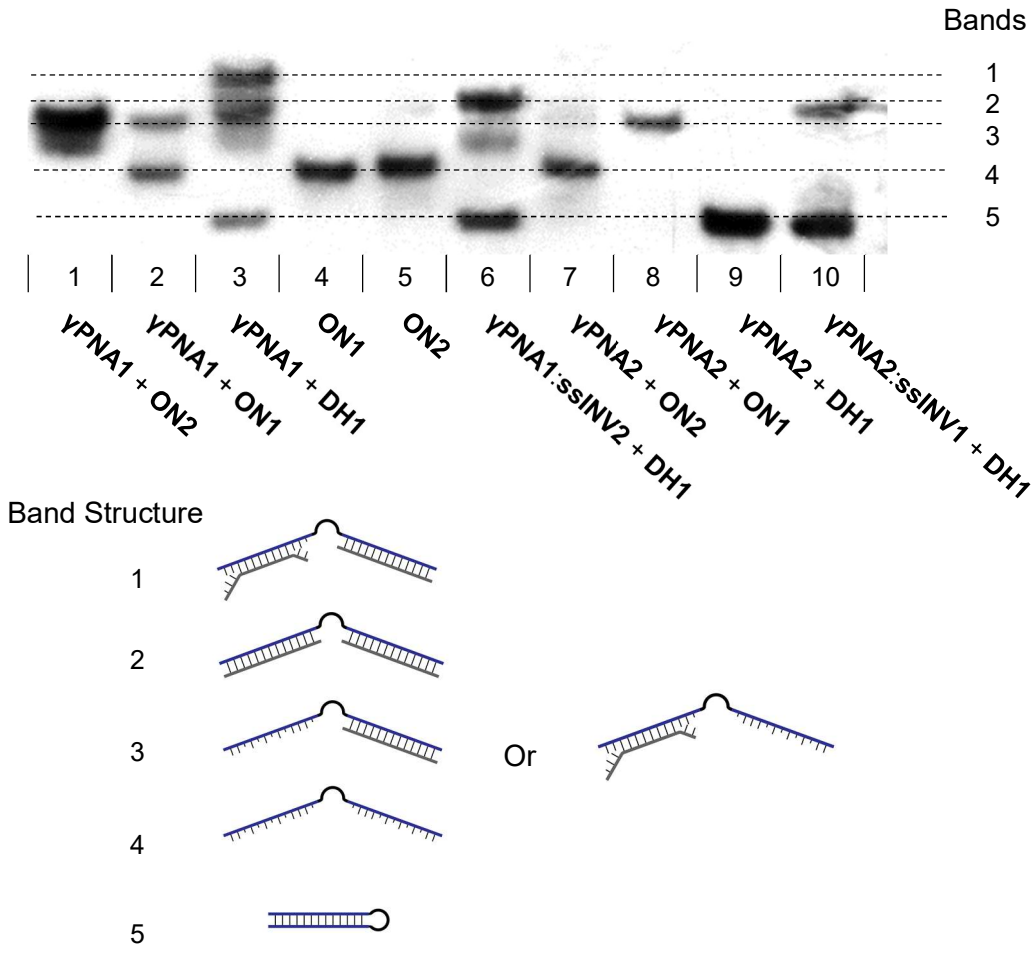

Figure S4. Representative electrophoretograms resolving incubation mixtures between a 5-fold molar excess of different probes and model dsDNA target **DH1** or linear targets **ON1** or **ON2** (34.4 mM) under annealing conditions. Probes and DNA targets were heated together (80 °C, 2 min), followed by cooling to room temperature over 30 min, and non-denaturing PAGE as described in Figure 5. **ON1**: 5'-GGT ATA TAT AGG CTT TTT TTT TTA ACT GAT CTA CTC; **ON2**: 5'-GAG TAG ATC AGT TTT TTT TTT TTG CCT ATA TAT ACC. Regions complementary to **γPNA2** (**ON1**) and **γPNA1** (**ON2**) are underlined.

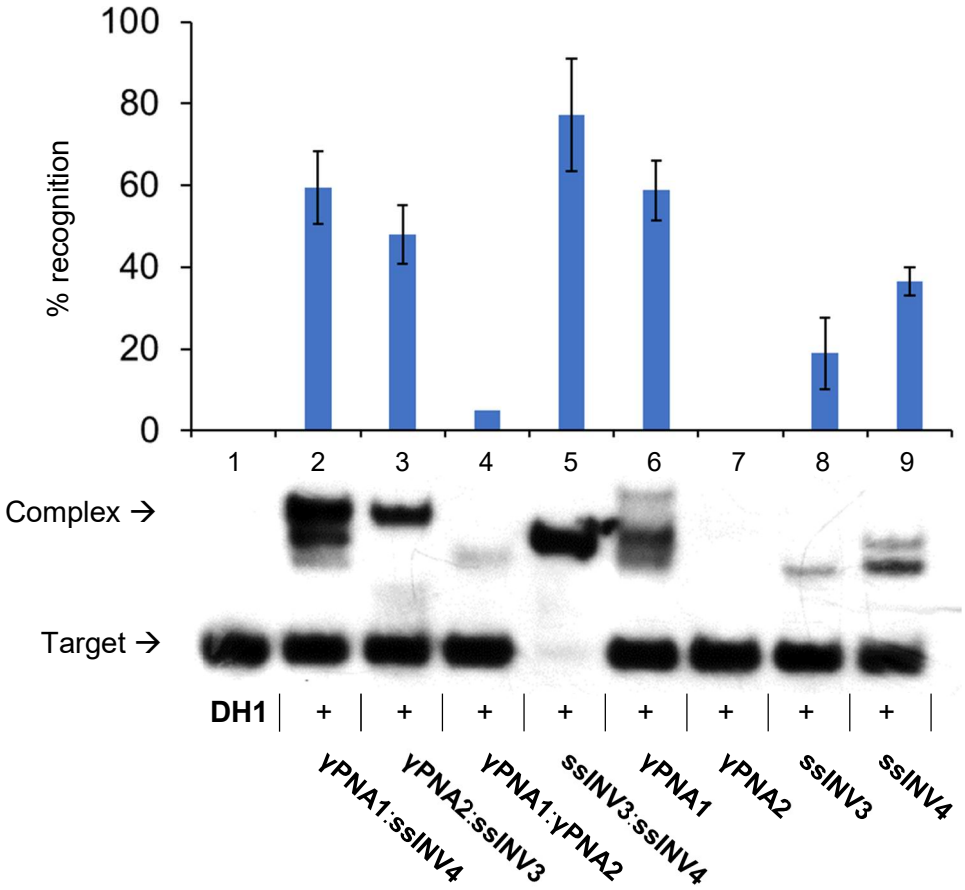

Figure S5. Representative electrophoretograms resolving incubation mixtures between model dsDNA target **DH1** and a 5-fold molar excess of chimeric γPNA-Invader, conventional Invader, single-stranded γPNA, or single-stranded Invader probes (37 °C, 2.5 h). Histograms depict averaged results from at least three experiments with error bars representing standard deviation. Conditions are as described in Figure 5.

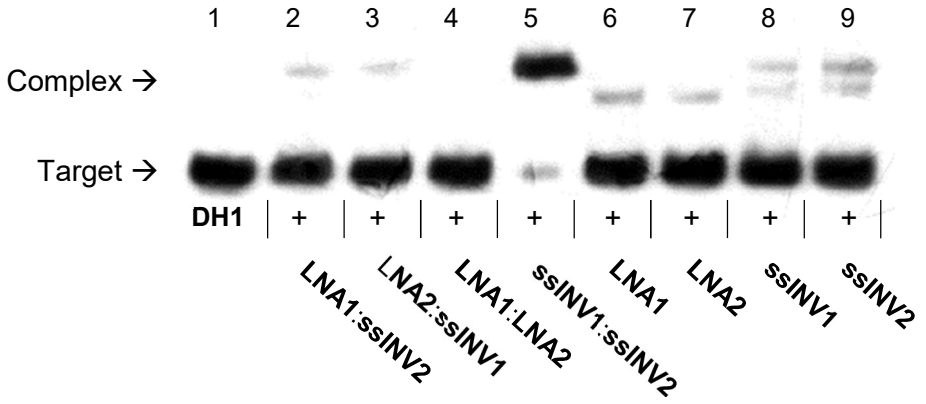

Figure S6. Representative electrophoretograms for recognition of model dsDNA target **DH1** (34.4 mM) using a 5-fold molar excess of chimeric LNA-Invader, conventional Invader, single-stranded LNA, or single-stranded Invader probes (37 °C for 2.5 h). Conditions are as described in Figure 5. Only minimal recognition of **DH1** is observed (<10%), except when conventional Invader probe **ssINV1**:**ssINV2** is used.

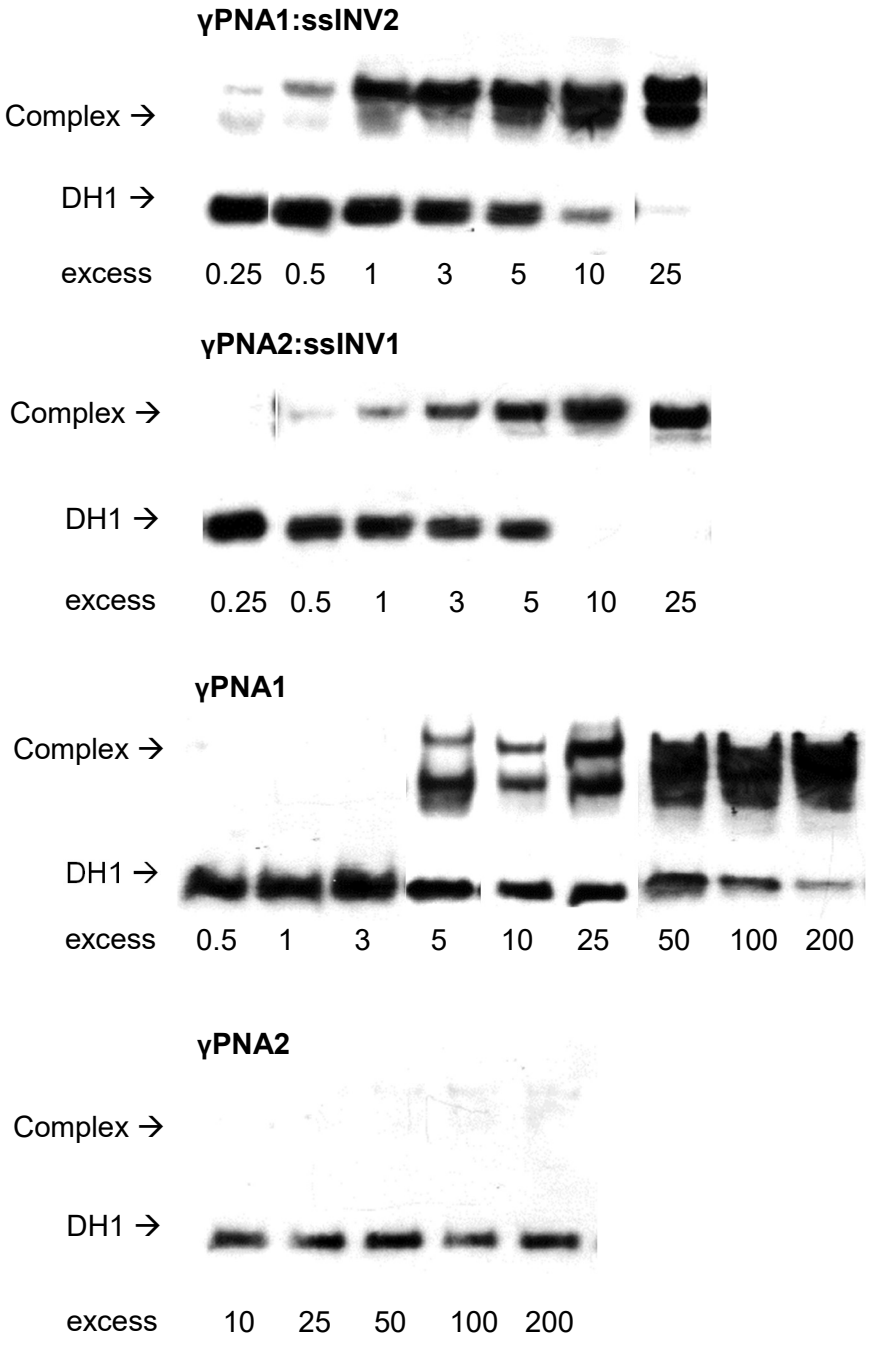

Figure S7. Dose-response experiments. Representative electrophoretograms for recognition of model dsDNA target **DH1** (34.4 mM) using different concentrations of chimeric γPNA-Invader probes and single-stranded γPNA probes at 37 °C for 2.5 hours. Conditions are as described in Figure 5. The electrophoretogram for **γPNA1** was previously reported in reference S2.

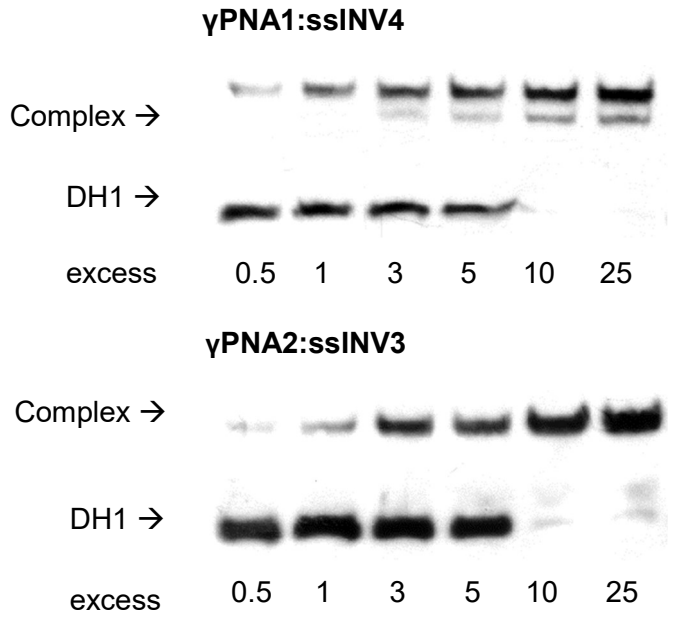

Figure S8. Dose-response experiments. Representative electrophoretograms for recognition of model dsDNA target **DH1** (34.4 mM) using different concentrations of chimeric γPNA-Invader probes at 37 °C for 2.5 hours. Conditions are as described in Figure 5.

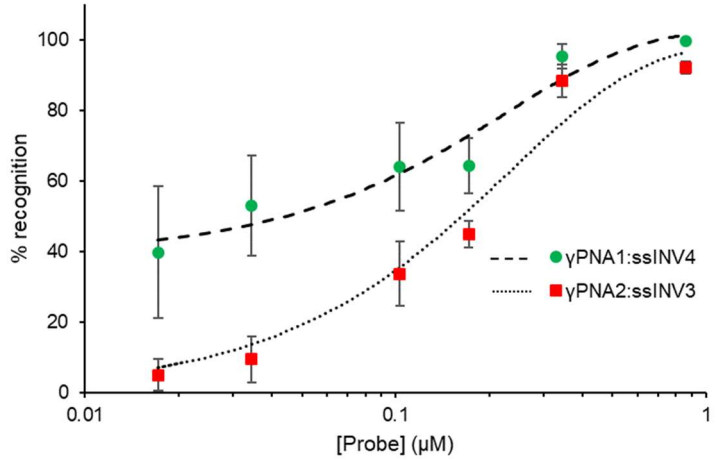

Figure S9. Dose-response curves for recognition of **DH1** using a subset of chimeric γPNA-Invader probes. Incubation conditions are as described in Figure 5 except that variable probe concentrations are used.

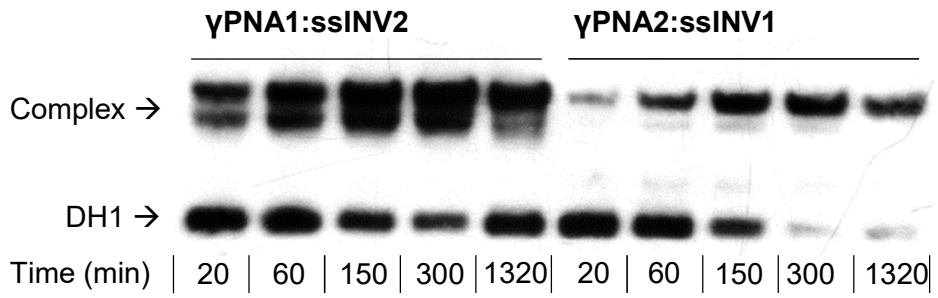

Figure S10. Time-course experiments. Representative electrophoretograms for recognition of model dsDNA target **DH1** (34.4 mM) using 5-fold molar excess of chimeric γPNA-Invader probes at 37 °C. Aliquots were taken at specific time points, flash-frozen in liquid N_2, and stored at -20 °C until analysis. Conditions are otherwise as described in Figure 5.

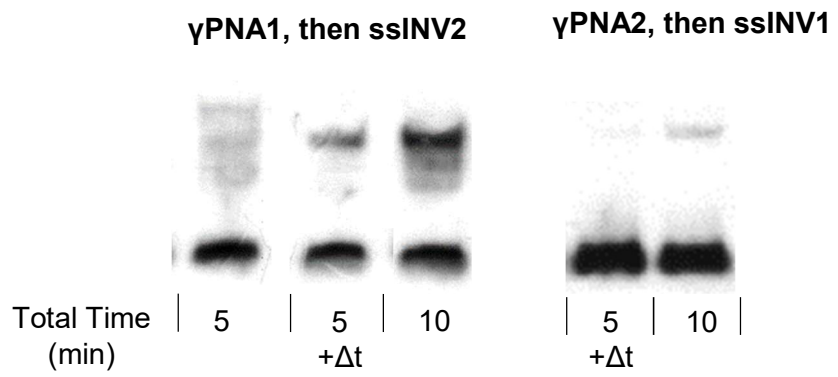

Figure S11. Additional experiments to probe recognition kinetics. **DH1** was incubated with **γPNA1** (left) or **γPNA2** (right) for 5 min, followed by addition of either **ssINV2** (left) or **ssINV1** (right), respectively, and incubation for the minimal time experimentally possible (Δt, i.e., time required to add and mix the corresponding individual Invader strand) or five additional minutes. Aliquots were taken at the specified time-points, flash-frozen in liquid N_2, and stored at -20 °C until analysis. Conditions are otherwise as described in Figure 5. As can be seen in the left panel, formation of recognition complexes - including the ternary **DH1**:(**γPNA1**)$_2$ complex – is rapid. Subsequent addition of **ssINV2** results in rapid formation of the **γPNA1**:**DH1**:**ssINV2** complex with no traces of the **DH1**:(**γPNA1**)$_2$ complex. This prompts us to speculate that recognition of **DH1** using the chimeric **γPNA1**:**ssINV2** probe is facilitated by rapid formation of catalytic amounts of ternary **DH1**:(**γPNA1**)$_2$ complex, which is transformed into the final **DH1**:**γPNA1**:**ssINV2** ternary complex. However, additional experiments are necessary to elucidate the mechanism.

Table S7. Sequences and T_m values of DNA hairpins used in this study.[a]

DH	Sequence	T_m (°C)
1		58.5
2		60.5
3		63.5
4		63.0
5		60.0
6		62.5
7		62.5

[a] For experimental conditions, see Table 1. Table previously reported in reference S3.

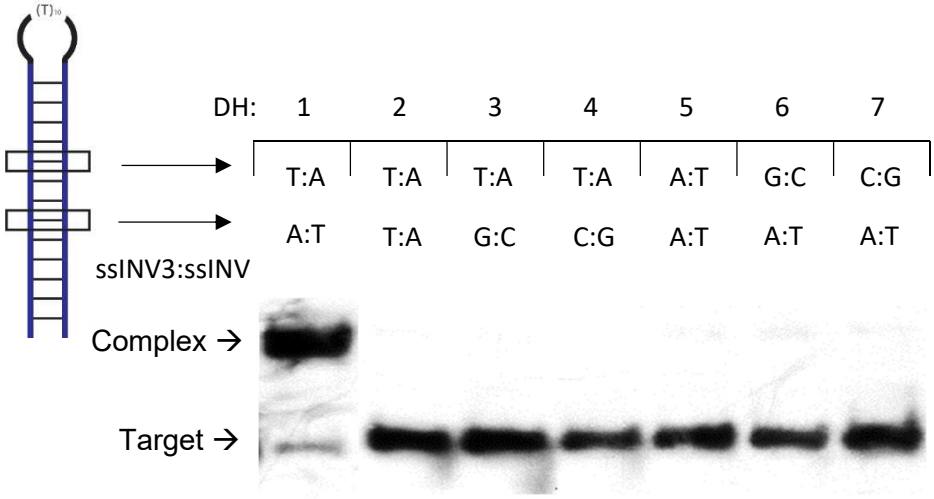

Figure S12. Binding specificity of conventional Invader probe **ssINV3:ssINV4** against non-complementary targets **DH2**-**DH7**. Representative electrophoretograms from experiments in which a 5-fold molar probe excess was incubated with **DH1**-**DH7** (34.4 nM) at 37 °C. Experimental conditions are as described in Fig. 5. For sequences and T_ms of **DH1**-**DH7**, see Table S7. The lanes have been rearranged to facilitate presentation but are from the same electropherogram. Data has been previously reported in reference S2 and are included for the reader's convenience.

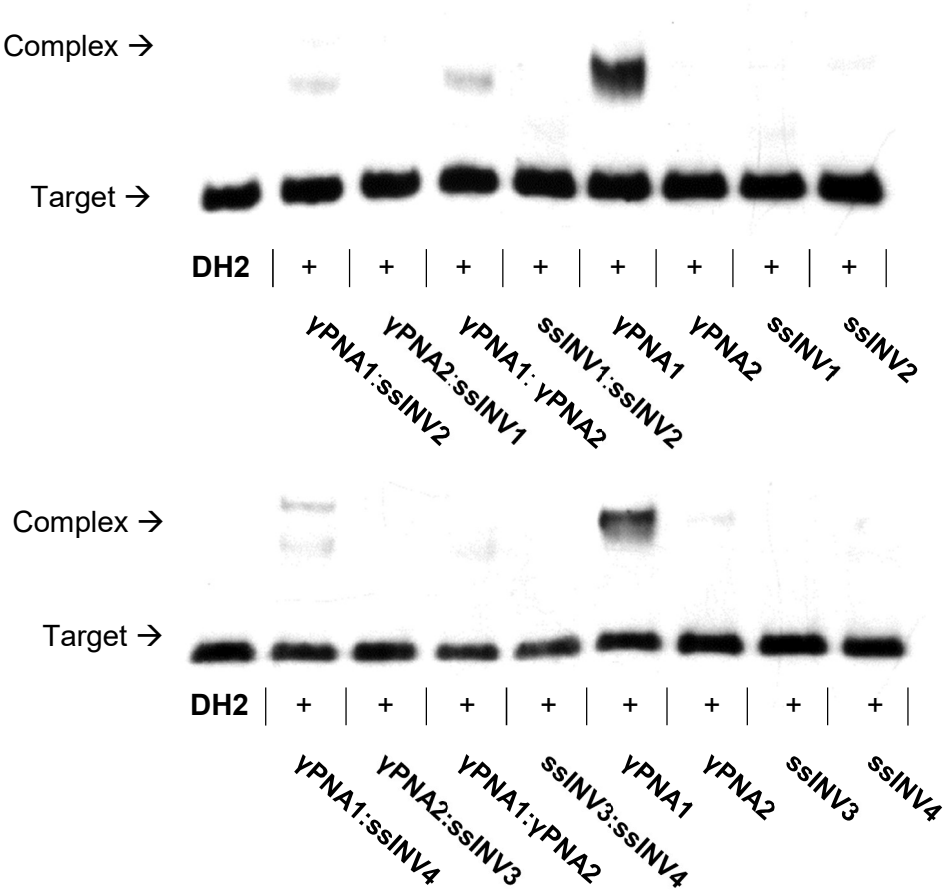

Figure S13. Additional binding specificity data. Representative electrophoretograms for recognition of model dsDNA target **DH2** (34.4 mM) using 5-fold excess of various probes at 37 °C for 2.5 h. Conditions are as described in Fig. 5.

Supplementary references

S1. V. V. Filichev, U. B. Christensen, E. B. Pedersen, B. R. Babu and J. Wengel, *ChemBioChem*, 2004, **5**, 1673-1679.

S2. R. Emehiser, E. Hall, D. C. Guenther, S. Karmakar and P. J. Hrdlicka, *Org. Biomol. Chem.*, 2020, **18**, 56-65.

S3. D. C. Guenther, G. H. Anderson, S. Karmakar, B. A. Anderson, B. A. Didion, W. Guo, J. P. Verstegen and P. J. Hrdlicka, *Chem. Sci.*, 2015, **6**, 5006-5015.